

Supporting Information

Separately enhanced dual emissions of amphiphilic derivative of 2-(2'-hydroxyphenyl) benzothiazole by supramolecular complexation

Chengfeng Wu, Yingzhi Jin, Dahua Li, Lan Ding, Yuzhi Xing, Kaicheng Zhang, and Bo Song*

College of Chemistry, Chemical Engineering and Materials Science
Soochow University, Ren-ai Road 199, 907-1341, 215123 Suzhou, P. R. China
E-mail: songbo@suda.edu.cn

1. The ^1H NMR and mass spectra of compounds.

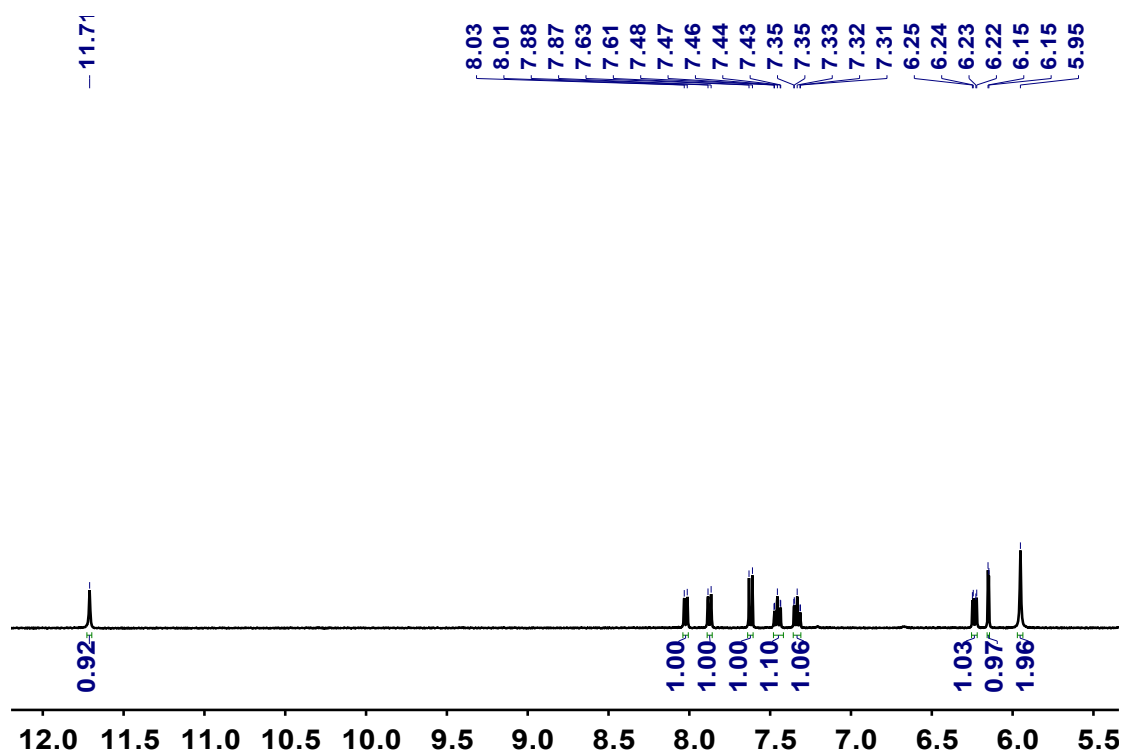


Fig. S1 Partial ^1H NMR spectrum (400 MHz, $\text{DMSO-}d_6$, 298 K) of compound A.

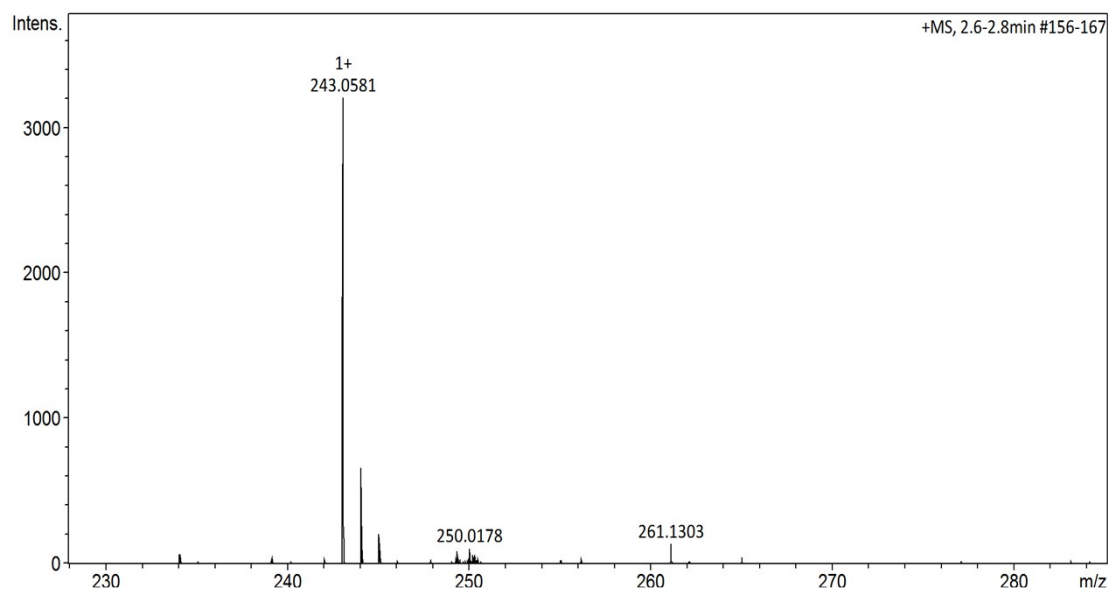


Fig. S2 Electrospray ionization mass spectrum of compound A. Assignment of the main peak: m/z 243.05 $[\text{A} + \text{H}]^+$.

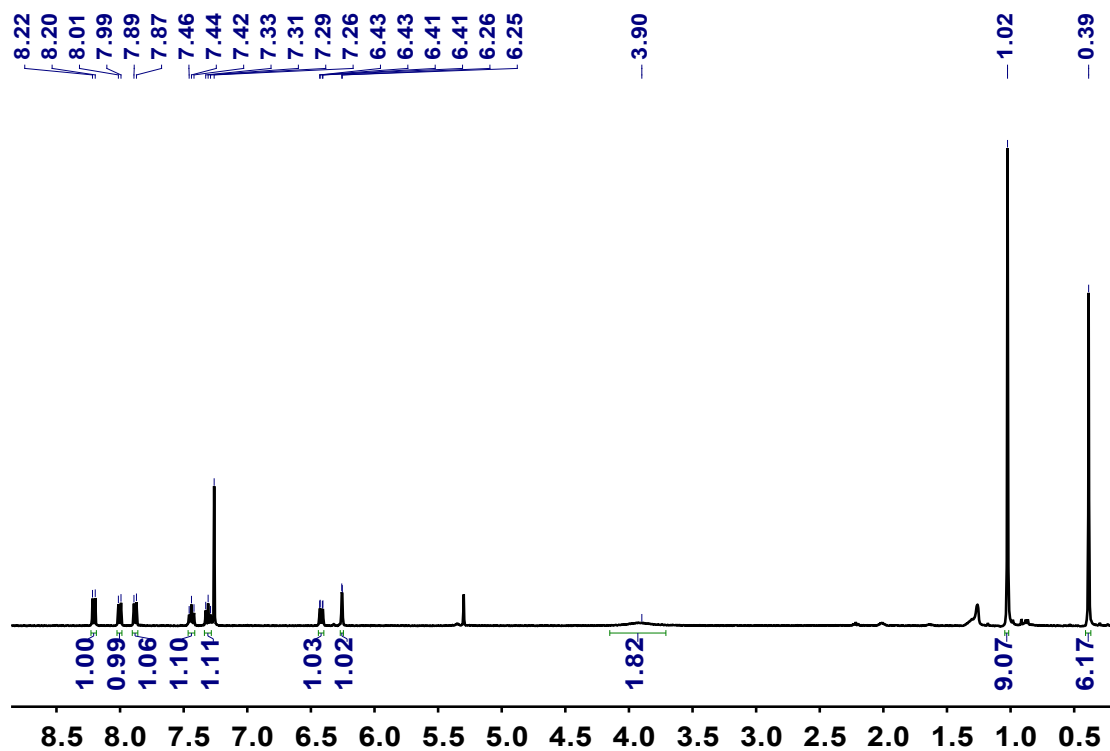


Fig. S3 Partial ^1H NMR spectrum (400 MHz, CDCl_3 , 298 K) of compound **B**.

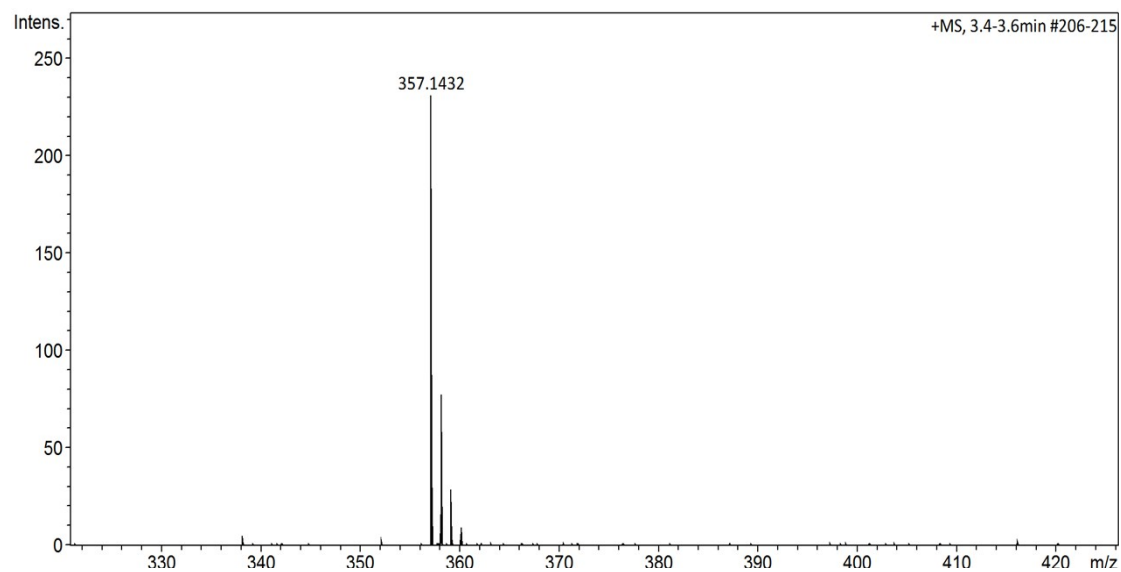


Fig. S4 Electrospray ionization mass spectrum of compound **B**. Assignment of the main peak: m/z 357.14 $[\text{B} + \text{H}]^+$.

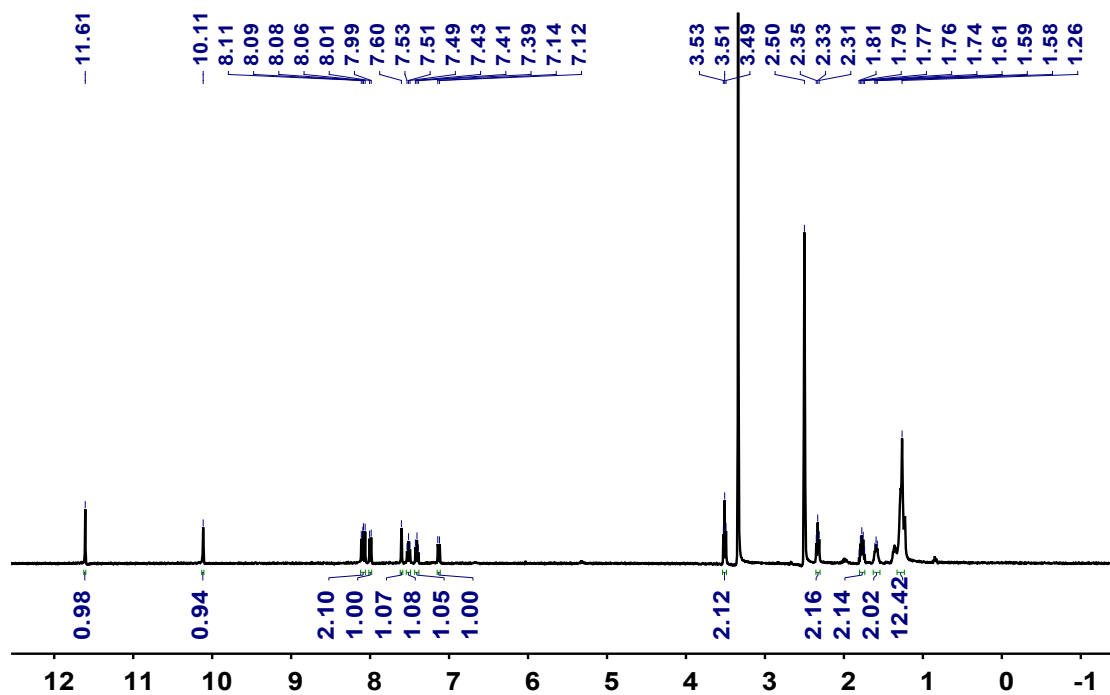


Fig. S5 ^1H NMR spectrum (400 MHz, $\text{DMSO-}d_6$, 298 K) of compound **C**.

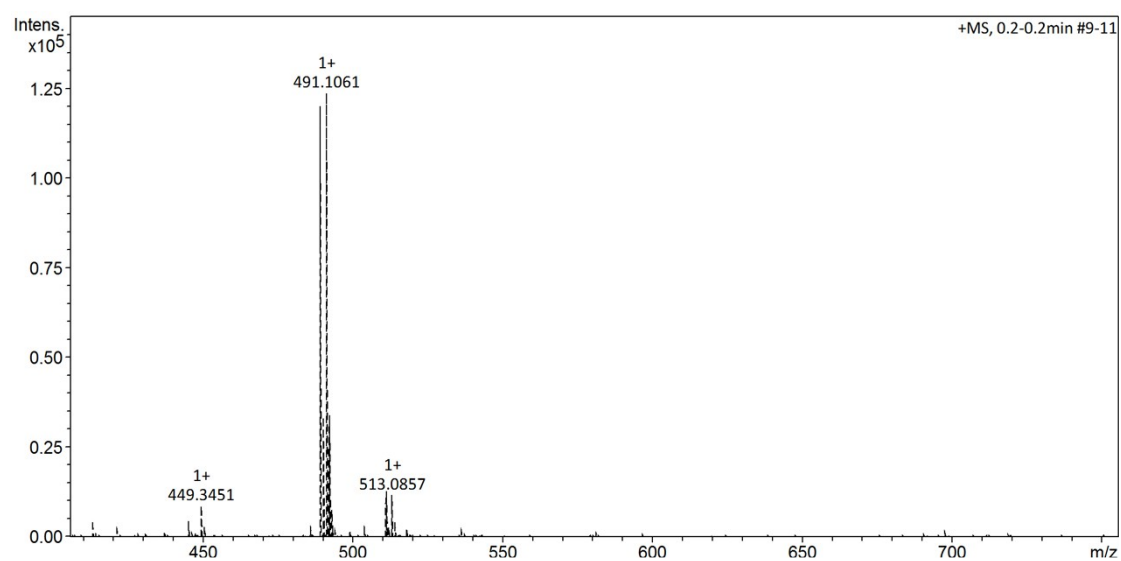


Fig. S6 Electrospray ionization mass spectrum of compound **C**. Assignment of the main peak: m/z 491.10 [**C** + H] $^+$.

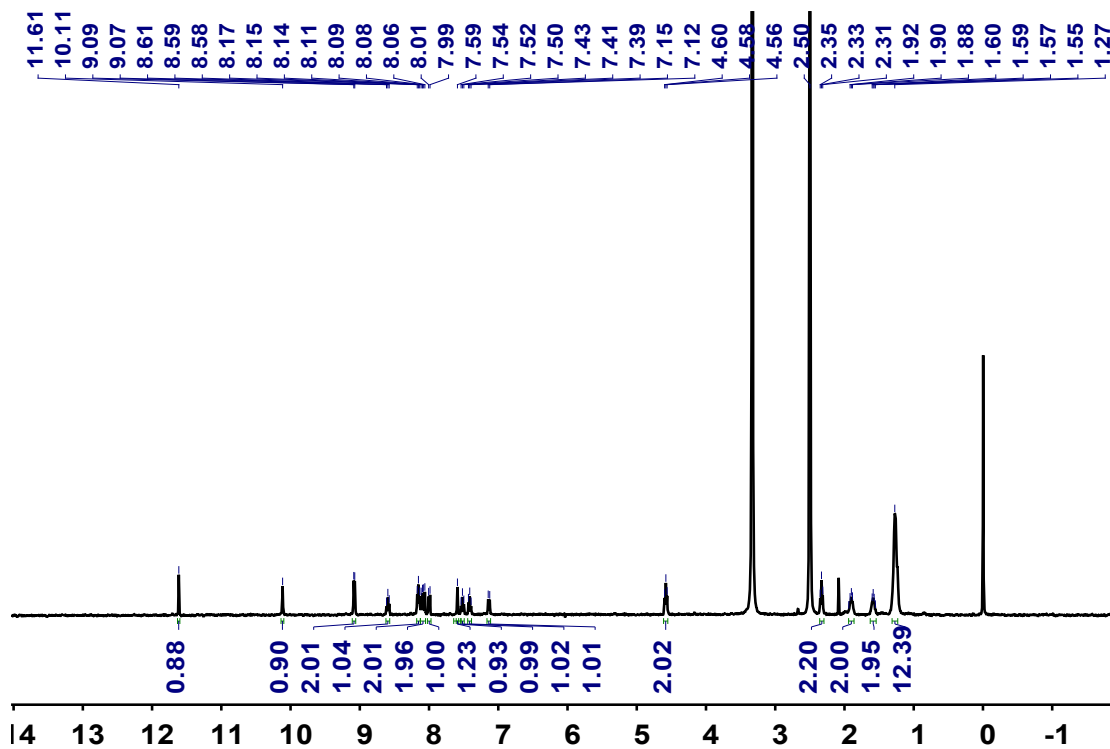


Fig. S7 ^1H NMR spectrum (400 MHz, $\text{DMSO-}d_6$, 298 K) of HBT-11.

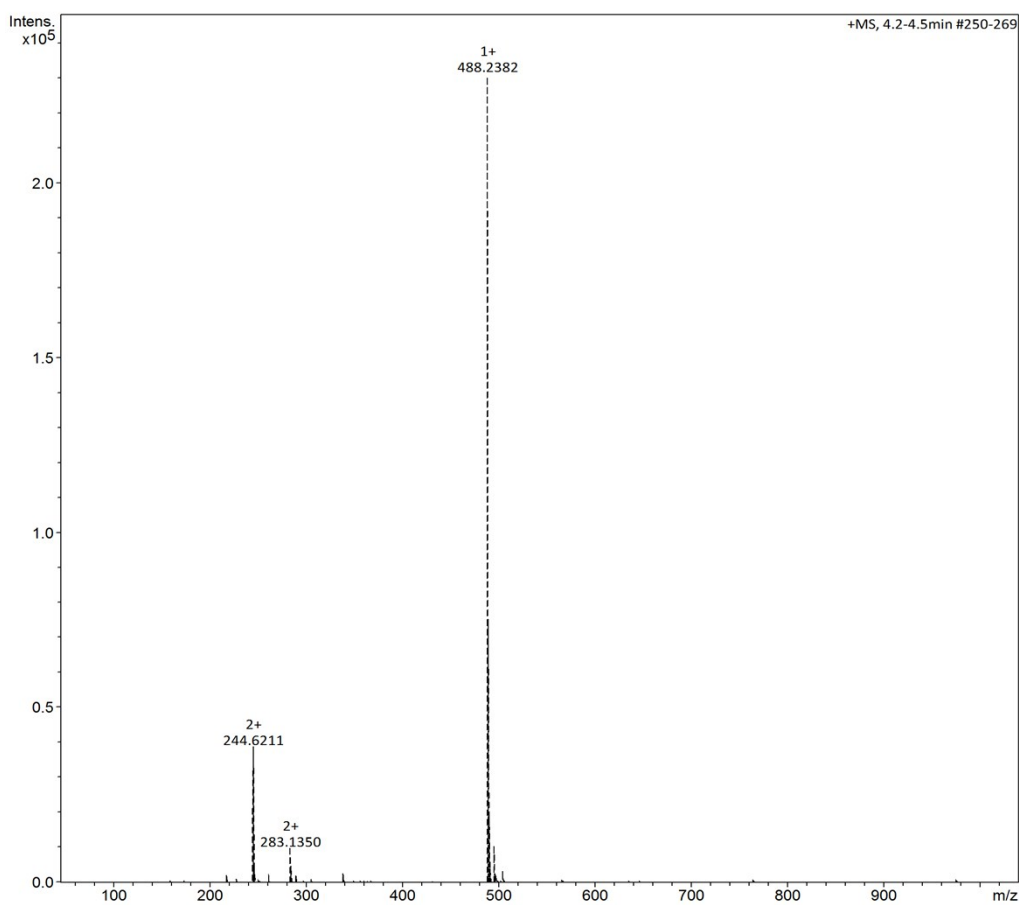


Fig. S8 Electrospray ionization mass spectrum of HBT-11. Assignment of the main peak: m/z 488.23 $[\text{HBT-11} - \text{Br}^-]^+$.

2. The four-level photo-cycle process

The ESIPT process requires an intramolecular hydrogen bond between the proton donor (-OH, -NH₂) and neighboring proton acceptor (-C=O, -N=) groups of the molecule. In the ground state, the enol-form is stable. Upon excitation, the redistribution of electronic charge results in fast proton transfer from the donor to acceptor via the intramolecular hydrogen bond, and the enol-form converted to keto-form (still excited state). The keto-form at excited state decay to ground state via irradiative (or non-irradiative) emission. Finally, the keto-form at ground state goes back to the enol-form via reversible proton transfer. The whole process involves four energy levels, and so called four-level photo-cycle process.

3. The photograph of powder



Fig. S9 Photograph showing the color of HBT-11 powder under illumination of 365 nm light.

4. The fluorescence spectra of different concentration for determination of CMC

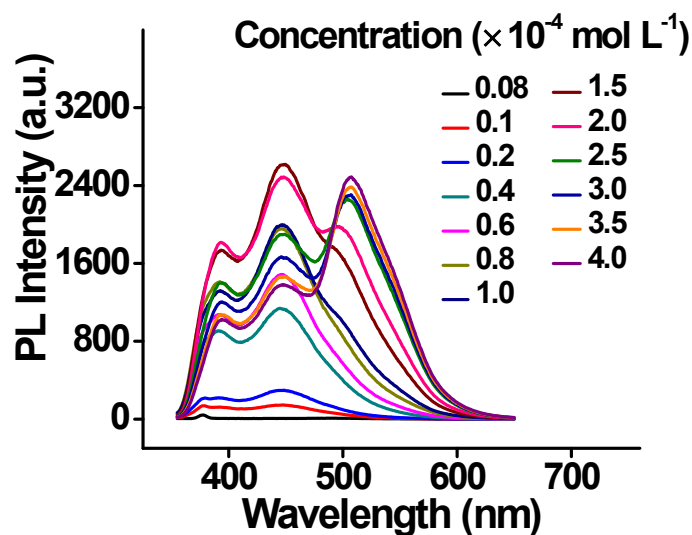


Fig. S10 Concentration-dependent fluorescence spectra of HBT-11 in aqueous solution. Curves represent 0.08×10^{-4} , 0.1×10^{-4} , 0.2×10^{-4} , 0.4×10^{-4} , 0.6×10^{-4} , 0.8×10^{-4} , 1.0×10^{-4} , 1.5×10^{-4} , 2.0×10^{-4} , 2.5×10^{-4} , 3.0×10^{-4} , 3.5×10^{-4} , 4.0×10^{-4} (mol/L).

5. The Tyndall effect of compound C in cyclohexane

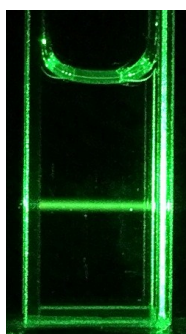


Fig. S11 The photograph of Tyndall effect for the cyclohexane solution of compound C.

6. The morphological change of HBT-11 upon addition of the two CDs

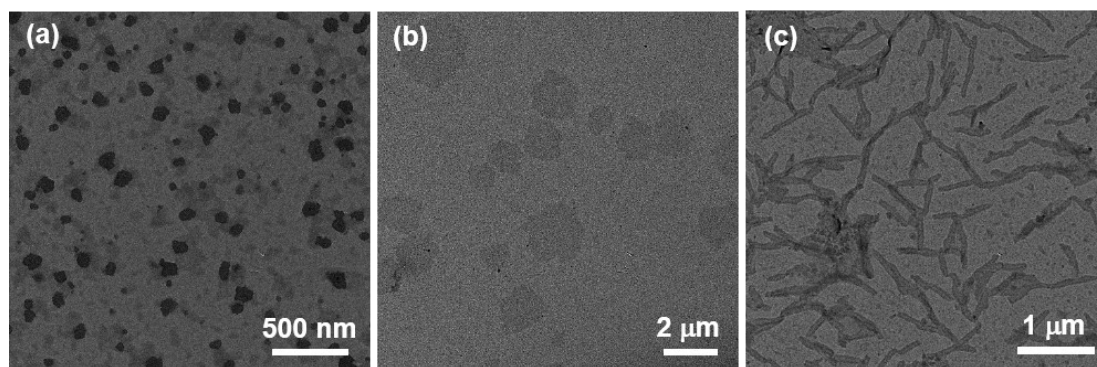


Fig. S12 The TEM images of (a) HBT-11 (4.0×10^{-4} mol/L), (b) HBT-11/ α -CD (1eq.), (c) HBT-11/ β -CD (1eq.).

7. The quantum yield of HBT-11 in different systems

Table S1 Quantum yield of HBT-11 in different concentrations in the absence and presence of CDs.

Concentration	System	Φ_F (%)
5.0×10^{-5} mol/L	HBT-11	1.0
	+ α -CD	3.7
	+ β -CD	3.4
4.0×10^{-4} mol/L	HBT-11	1.1
	+ α -CD	4.1
	+ β -CD	3.4

8. The time-resolved fluorescence of HBT-11 in different systems

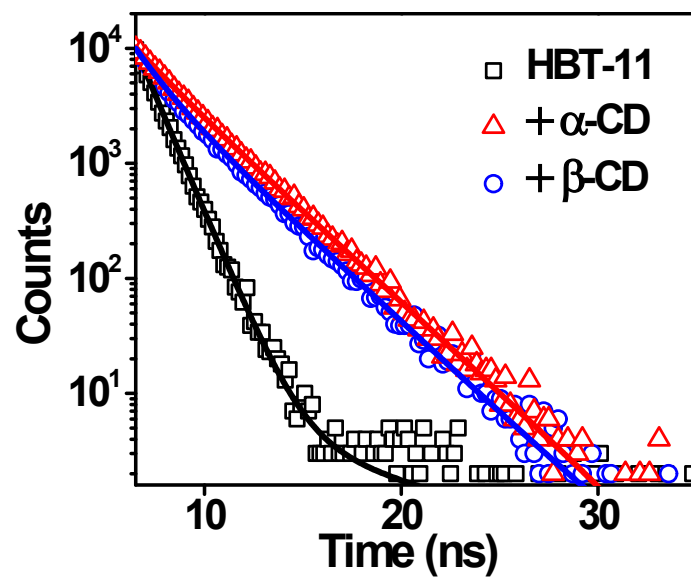


Fig. S13 Time-resolved fluorescence decays of HBT-11 in the absent and presence of α -CD and β -CD in aqueous solution.